BULETINUL INSTITUTULUI POLITEHNIC DIN IAŞI
Publicat de
Universitatea Tehnică „Gheorghe Asachi” din Iaşi
Volumul 65 (69), Numărul 4, 2019
Secţia
MATEMATICĂ. MECANICĂ TEORETICĂ. FIZICĂ

THE IMPACT OF MATHEMATICAL QUANTIFICATIONS OF RADIOTRACER CELLULAR UPTAKE IN FUNCTIONAL IMAGING

BY

WAEL JALLOUL[1,2], VLAD GHIZDOVĂȚ[2,*], IRENA CRISTINA GRIEROSU[1,2] and CIPRIANA ȘTEFĂNESCU[1,2]

[1]Nuclear Medicine Laboratory, “Sf. Spiridon” County Emergency Hospital, Iași, Romania
[2]“Grigore T. Popa” University of Medicine and Pharmacy, Iași, Romania,
Faculty of Medicine, Biophysics and Medical Physics Department

Received: November 18, 2019
Accepted for publication: December 17, 2019

Abstract. The combination between personalised image acquisition protocols (in completion to the standard protocols), the good understanding of radiotracer cellular uptake mechanisms, and the use of the appropriate mathematical algorithm for the quantification of radiopharmaceutical uptake, is very important to avoid “the naive image reading” in nuclear functional imaging.

Starting from the study of ^{99m}Tc-sestaMIBI uptake mechanisms, we aimed to demonstrate that this combination is necessary to reach a mindfull interpretation of images, especially in the case of intricated pathologies.

Keywords: quantifications; radiotracer; uptake; ^{99m}Tc-sestaMIBI; functional imaging.

1. Introduction

In nuclear imaging, tissue function is directly proportional to the measurement of radiotracer cellular uptake (high uptake - hyperfunctional tissue, low uptake - hypofunctional tissue, normal uptake - normal functional

*Corresponding author; *e-mail*: vlad.ghizdovat@gmail.com

tissue) and its distribution (uniformity, heterogeneity). That is why the mindfull interpretation of functional images is based specially on the good understanding of radiotracer cellular uptake mechanisms and its quantification methods, in order to avoid "the naive image reading".

Beginning with the study of ^{99m}Tc-sestaMIBI uptake mechanisms, we aimed to demonstrate the importance of the use of appropriate mathematical algorithms and processing methods in radiotracer uptake quantification.

2. Materials and Methods

^{99m}Tc-sestaMIBI is the most important representative of ^{99m}Tc-isonitrile radiotracers, often indicated in parathyroid (Redman *et al*., 2019), myocardial and oncological scans. Its essential feature, is the presence of sixth alkyl group in the terminal position, which creates a "lipophilic sphere" around the metal atom, and allows free crossing of the hydrophobic environment of the membrane lipid bilayer (Fig. 1) (Piwnica-Worms and Holman, 1990).

^{99m}Tc-sestaMIBI passive transport is performed after the simple diffusion pattern of a lipophilic molecule, requiring more energy than the diffusion facilitated by a carrier. The transport is done in the electrochemical gradient direction, and is based on Nernst equations (Fig. 2) (Ștefănescu *et al*., 1996).

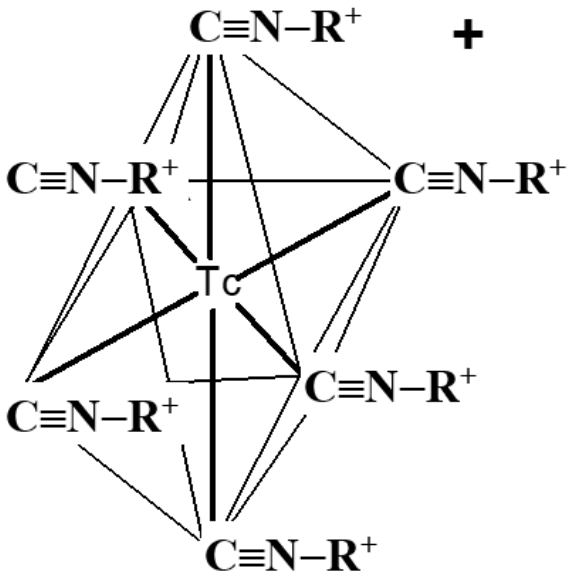

Fig. 1 – "Lipophilic sphere" resulting from the octahedral configuration of the isonitrile molecule (3). In the case of sestaMIBI, R corresponds to the radical: $CH_2C(CH_3)_2OCH_3$.

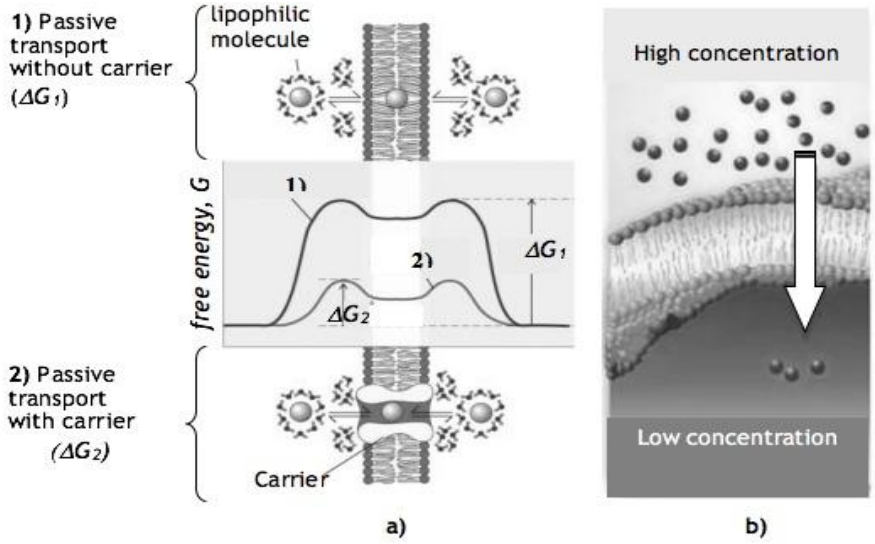

Fig. 2 – ^{99m}Tc-MIBI passive transport is performed like the simple diffusion pattern of a lipophilic molecule, requiring more energy than the diffusion facilitated by a carrier (*a*). The transport is done in the electrochemical gradient direction (*b*).

The radioactive molecule presents a single positive global electrical charge, delocalized, which determines the passage through the membrane depending on the membrane potential, as demonstrated by the following equations (Ștefănescu and Rusu, 2007):

$$\begin{aligned} &\left(Tc-MIBI\right)_{cit}=\left(Tc-MIBI\right)_{ext}e^{-\left(\Delta\Phi_{pl}\right)/F/RT}\\ &\Delta\Phi_{pl}=\frac{RT}{zF}\ln\frac{\left(Tc-MIBI\right)_{ext}}{\left(Tc-MIBI\right)_{cit}}\\ &\text{or}\\ &\Delta\Phi_{pl}=2.3\frac{RT}{zF}\log_{10}\frac{\left(Tc-MIBI\right)_{ext}}{\left(Tc-MIBI\right)_{cit}} \end{aligned} \tag{2}$$

However, $2.3RT/zF\cong 60$ mV for a monovalent ion at room temperature, such that

$$\left(Tc-MIBI\right)_{cit}=\left(Tc-MIBI\right)_{ext}10^{-\left(\Delta\Phi_{pl}\right)/60} \tag{3}$$

where $\Delta\Phi_{pl}$ is the plasma membrane potential, $\left(Tc-MIBI\right)_{ext}$ is the ^{99m}Tc-sestaMIBI extracellular concentration, $\left(Tc-MIBI\right)_{ext}$ is the

^{99m}Tc-sestaMIBI intracytoplasmatic concentration, and RT/zF is a constant, with z – number of electrons transferred per mole, F – Faraday's number, R – gas constant, and T – absolute temperature.

The intracytoplasmic concentration of ^{99m}Tc-sestaMIBI, was determined to be five times higher than its extracellular concentration (Piwnica-Worms and Holman, 1990).

After entering the cytoplasm, the radiotracer crosses the mitochondrial membrane and accumulates in the mitochondria, according to the following Nernst equation:

$$(Tc-MIBI)_{mit} = (Tc-MIBI)_{cit}\, 10^{-(\Delta\Phi_{mit})/60} \tag{4}$$

where $\Delta\Phi_{mit}$ is the mitochondrial membrane potential and $(Tc-MIBI)_{cit}$ is the ^{99m}Tc-MIBI intra-mitochondrial concentration.

This intramitochondrial accumulation may exceed 300 times the cytosolic concentration; it depends on rest membrane potential of both plasma and mitochondria. In this sense, the previous equation can also be written:

$$(Tc-MIBI)_{mit} = (Tc-MIBI)_{ext}\, 10^{-(\Delta\Phi_{pl}+\Delta\Phi_{mit})/60} \tag{5}$$

Therefore, the ^{99m}Tc-sestaMIBI intramitochondrial distribution is approximately 90%, comparative to only 10% in the cytoplasm.

The ^{99m}Tc-MIBI cellular efflux is mediated by an integral plasmatic protein, MDR1-P glycoprotein (Pgp, see Fig. 3). ATP (adenosine triphosphate) depletion results in increased 99mTc-sestaMIBI accumulation from 40% to 90%, due to Pgp dependence on intracellular ATP concentration (Gupta *et al*., 2007; Mehta *et al*., 2005).

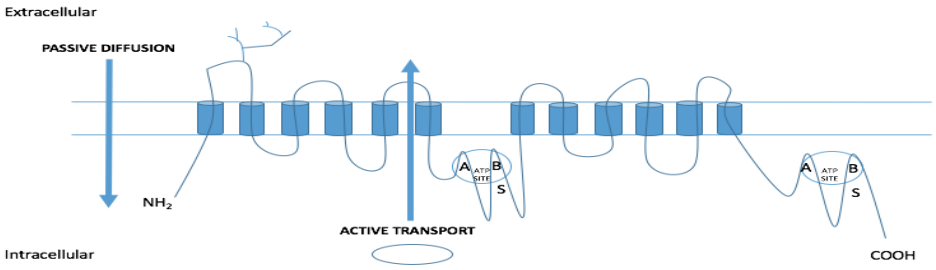

Fig. 3 – Schematic representation of ^{99m}Tc isonitrile efflux protein (Pgp).

Uptake in myocardial cells is often used for comparison in quantification. This is because myocardial cells have the most active mitochondria between normal cells, while epithelial cells and lymphocytes have the lowest mitochondrial activity (the uptake of ^{99m}Tc-sestaMIBI in myocytes

is nearly 10 times higher than in other cells). Normal epithelial cells have small mitochondrial potentials and as a result, perform a reduced capture for certain cationic lipophilic molecules (Ștefănescu and Rusu, 2007; Piwnica-Worms and Holman, 1990).

3. Results and Discussions

All these characteristics and equations can provide support for Nuclear Medicine specialistis in developing acquisition protocols (Ștefănescu *et al.*, 2016). For example, knowing that ^{99m}Tc-sestaMIBI parathyroid accumulation begins 4-6 minutes after administration (according to the short influx time), early images are able to be made after 15-20 minutes. In the case of tumor and depending on the degree of malignancy, the maximum uptake is described at 60 minutes and not at 120 minutes, like is the case of parathyroid adenoma demonstrated on delayed images (Carpentier *et al*., 1998).

An example of paraclinical use of a combination between mathematical algorithms and personalized acquisition protocols is about the quantification of myocardial 99mTc-Sestamibi uptake during experimental validation in a Porcine Model. Taking into account the changing activity of the radiotracer during the measurements which were obtained at different times, and the biologic washout, a correction algorithm was used.

To determine the biologic half-life, T_{biol}, of ^{99m}Tc-sestamibi in the porcine myocardium, a series of anterior planar images were acquired at specific times. A Region of Interest (ROI) was drawn around the myocardium on the planar image and the integral counts within this region of interest were determined for each dataset.

Then, by plotting the integral counts, *N*, within the myocardial region of interest as a function of time, *t*, it was possible to determine T_{biol} by fitting the data to:

$$N = N_0 e^{\left[-\ln(2)\left(t/T_{phys}\right)\right]} e^{\left[-\ln(2)\left(t/T_{phys}\right)\right]} \tag{6}$$

where N_0 is a normalization factor and is the physical half-life of ^{99m}Tc (*i.e.*, 6 h).

Another type of absolute Focal Tracer Uptake Calculation using correction algorithms can be derived from performed 3D single-photon emission computed tomography (SPECT)/computed tomography (CT) myocardial images. After the corrections for extracardiac activity and partial-volume errors, the total counts of targeted radiotracer uptake in the segmented left ventricular (LV) myocardium are normalized by the total counts of the external point source – Eq. (7). The radiotracer uptake is in turn weighted by the known radioactivity of the external point source to yield absolute radiotracer

uptake (Da Silva *et al*., 2001). The total radiotracer uptake is thus calculated by (Li *et al*., 2005; Li *et al*., 2013)

$$\text{Targeted radiotracer uptake} = \frac{\iiint V_{LV}\zeta(v)dv}{\iiint V_{PS}\,p(u)du}c \tag{7}$$

where $\zeta(v)$ denotes the targeted radioactivity in the segmented LV miocardial voxel v, $p(u)$ denotes the radioactivity in the point source voxel u, c is the known radioactivity in the point source, V_{LV} and V_{PS} represent the total volumes of the LV myocardium and the point source, respectively.

4. Conclusions

The main conclusions of the present paper are the following:

i) Acquisition protocols are designed so they could be used to confirm the structure and performance of the algorithm. Mathematical algorithms depend on the type of quantification needed, the radiotracer uptake mechanisms, the type of images performed (planar images or SPECT images), the type of tissue investigated etc. Preclinical models play a crucial role in developing personalized algorithms for the measurement of the radiotracer uptake.

ii) Quantification and even uptake graphs of the radiopharmaceutical over time can provide important arguments about differential diagnosis of benign/malignant, for example in the case of thyroid node/parathyroid adenoma. That is why it is very important to choose the most suitable acquisition protocol and mathematical algorithm for a good measuement of cellular uptake in order to have a better idea about the tissular function.

iii) For taking into consideration the decrease of radiotracer activity in time, the uptake mechanisms, the thickness of the investigated tissue and errors that may occur during image acquisition, mathematical algorithms represent an important tool for radiotracer uptake quantification and then for a better interpretation of images, reaching a crucial understanding of the function of examined tissues.

REFERENCES

Carpentier A., Jeannotte S., Verreault J. *et al*., *Preoperative Localization of Parathyroid Lesions in Hyperparathyroidism: Relationship Between Technetium-99m-MIBI Uptake and Oxiphil Cell Content*, J. Nucl. Med., **39**, 1441-1444 (1998).

Da Silva A.J., Tang H.R., Wong K.H. *et al*., *Absolute Quantification of Regional Myocardial Uptake of 99mTc-Sestamibi with SPECT: Experimental Validation in a Porcine Model*, J. Nucl. Med., **42**, 772–779 (2001).

Gupta Y., Ahmed R., Happerfield L. *et al*., *P-Glycoprotein Expression is Associated with Sestamibi Washout in Primary Hyperparathyroidism*, Br. J. Surg., **94**, 1491-1495 (2007).

Li S., Dobrucki L.W., Sinusas A.J., Liu Y.-H., *A New Method for SPECT Quantification of Targeted Radiotracers Uptake in the Myocardium*, Med. Image Comput. Assist. Interv., **8**, 684-691 (2005).

Li S., Sinusas A.J., Dobrucki L.W., Liu Y.-H., *New Approach to Quantification of Molecularly Targeted Radiotracer Uptake from Hybrid Cardiac SPECT/CT: Methodology and Validation*, J. Nucl. Med., **54**, 2175-2181 (2013).

Mehta N.Y., Ruda J.M., Kapadia S. *et al*., *Relationship of Technetium Tc 99m Sestamibi Scans to Histopathological Features of Hyperfunctioning Parathyroid Tissue*, Arch. Otolaryngol. - Head and Neck Surg., **131**, 493-498 (2005).

Redman S., Graham R., Little D., *British Nuclear Medicine Society Clinical Guideline for Parathyroid Scintigraphy*, 1-9, https://www.bnms.org.uk/ (2019).

Piwnica-Worms D., Holman B.L., *Noncardiacaplications of Hexakis (Alkyl Isonitril) Technetium-99m Complexes*, J. Nucl. Med., **31**, 1166-1167 (1990).

Ștefănescu C., Chaussiere L., Rusu V. *et al*., *Explorări scintigrafice complementare (99mTc MDP, 99mTc MIBI şi Octreoscan) în evaluarea neoplasmului mamar*, Rev. Med. Chir. Soc. Med. Nat., **100**, in Romanian, 165-168 (1996).

Ștefănescu C., Ionescu L., Dănilă R. *et al*., *Tc-99m Mibi Thymic Scintigraphy in Diagnosis and Therapeutic Decision Making: What Is Behind the Image?*, Acta Endocrinologica, **12**, 249-256 (2016).

Ștefănescu C., Rusu V., *From Radiopharmaceuticals to Functional and Molecular Imaging*, Technopress, Iași, 2007.

IMPACTUL CUANTIFICĂRILOR MATEMATICE ALE CAPTĂRII CELULARE A RADIOTRASORULUI ÎN IMAGISTICA FUNCȚIONALĂ

(Rezumat)

Combinația dintre protocoalele de achiziție de imagini personalizate (completând ghidurile standardizate), buna înțelegere a mecanismelor de captare celulară a radiotrasorului și utilizarea algoritmilor matematici adecvați pentru cuantificarea captării radiofarmaceuticului, este foarte importantă pentru a evita „citirea naivă a imaginilor”, în imagistica nucleara funcțională.

În prezenta lucrare ne-am propus să demonstrăm, pornind de la studiul mecanismelor de captare a ^{99m}Tc-sestaMIBI, că această combinație este necesară pentru a ajunge la o interpretare cât mai corectă a imaginilor, în special în cazul patologiilor complexe.